# GREEN CHEMISTRY: CARBON-BEARING MINERALS AS A SOURCE OF NANOCARBONS

Prof. Huczko A.[*1], Dr Dąbrowska A.[1], Dr Fronczak M.[1], Dr Strachowski P.[1], Sokołowski S.[1], Prof. Bystrzejewski M.[1], Prof. Subedi D.P. [2], Dr Kafle B.P.[2]

Department of Chemistry, Warsaw University, Warsaw, Poland[1]

School of Science, Kathmandu University, Dhulikhel, Kavre, Nepal[2]

[*]ahuczko@chem.uw.edu.pl

***Abstract:*** *Natural abundant, cheap and widely used raw materials like calcite, magnesite and dolomite contain elemental carbon up to several wt percent. Such rocks have been chemically processed here using combustion synthesis route to yield novel nanocarbons including two-dimensional graphene-like structures. The fast and efficient reduction of powdered minerals with strong reducer (Mg) produces, after chemical wet purification, carbon nanomaterial which was analyzed using different techniques like XRD and SEM. This 'combustion' process was followed on-line to evaluate reaction duration (usually within 1 sec).*

**Keywords**: COMBUSTION SYNTHESIS, CARBOB-BEARING MINERALS, NANOCARBONS

## *1. Introduction*

Carbon is one of the most important elements in the world as it builds both organic and inorganic matter. Till XX century only two allotropes of carbon were known, graphite and diamond (in addition to amorphous carbon, i.e. soot or carbon black). Recent decades brought into a daylight, however, new nanocarbon allotropes[1]. In 1985 the fullerenes were discovered[2], with the importance of the discovery honored with a Nobel Price (1996). Soon later, carbon nanotubes (even called the 'black diamonds of XX century') were shown to the world (1991)[3]. The very beginning of the XXI century brought one, even more important discovery of next new carbon allotrope – graphene[4]. Graphene and graphene-related nanomaterials are indeed a revolutionary materials. They have many applications replacing conventional materials as well as the ability to support applications previously not possible before the advent of two-dimensional materials. The applications of graphene are truly endless and many are yet to be conceived of[5].

Essentially, the nanomaterials are synthesized using either 'top-down' (miniaturization) or 'bottom-up' approach. The latter one makes the use of the smallest 'building blocks' (atoms, ions and molecules) which form nanostructures via coalescence and coagulation during quench. Those starting promoters are usually produced via high-energy activation of a bulk material (i.e. plasma, laser or high-temperature activation). Dyjak et al.[6] synthesized an intriguing carbon nitride $C_3N_4$ via high-temperature pyrolysis of melamine. In a search for novel nanocarbons, Manning et al.[7] prepared the exfoliated graphite (in minuscule, however, amounts) from fluorinated graphite already in 1999 using inductively coupled Ar plasma. High energy consumption is, however, a drawback of the listed routes.

Here we propose a SHS (Self-propagating High-temperature Synthesis) approach for the formation of nanocarbons. SHS also termed combustion synthesis (CS) is a strong high-temperature, exothermic and autothermic, and fast redox reaction that leads to the formation of new thermodynamically stable nanomaterials with structures often not obtained under conventional conditions[8]. We reported earlier[9] that silicon carbide nanowires were efficiently synthesized via silicon-polytetrafluoroethene thermolysis. Later on, the solid carbon nanomaterials were successfully obtained using the reduction of different carbon-bearing compounds. Thus, Dąbrowska et al.[10] atomized different carbonates by using strong reducers to obtain novel nanomaterials. Such research was later continued towards the heterogeneous autothermic reduction of $CO_2$ and CO to elements using the following reducers: Li, Mg, Ca, B, Ti, Zr, and Al[11]. The solid product contained the layered graphite and nanocarbides. Novel carbon nanostructures were also obtained by Huczko et al.[12] from the mixtures of strong metal reducers and strong oxidizers (fluorinated graphite, TEFLON®, PTFE and PVC). Few-layered graphene was also produced via reduction of graphite oxide and fluorinated graphite using different reducers[13]. Recently, Dyjak et al.[14] prepared porous graphenic nanomaterials through a self-sustaining magnesiothermic reduction of oxalic acid.

Here, we've extended such research into a field of 'Green Chemistry' – processing of cheap and abundant minerals (which contain elemental carbon) via combustion synthesis. Specifically, the minerals (natural carbonates) of Polish and Nepal origin were chosen as oxidants with a relatively high content of elemental carbon. A phthalic acid, as a pure carbon-bearing reference reactant, was also reduced with magnesium.

## *2. Experimental*

The reduction of carbon-bearing compounds was carried out in the stainless-steel high-pressure vessel (volume 375 $cm^3$, Fig. 1) following the protocol outlined earlier[9]. The reactor (a modified bomb calorimeter) is resistant to extreme process parameters (very high temperature, pressure gradients, and chemically aggressive reaction environment) and was pre-tested at the pressure up to 10 MPa.

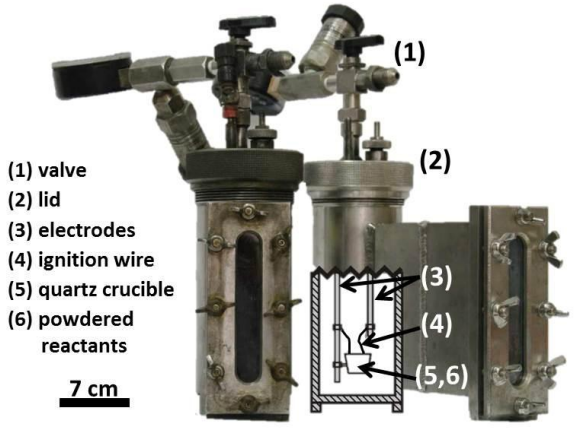


***Fig. 1****. Modified bomb calorimeter as a CS reactor*

A stoichiometric mixture of the reactants (Mg powder/carbon-bearing oxidant) was powdered and loaded into the quartz crucible under the pre-planned atmosphere (Ar) and pressure. The reaction was started by the resistive heating of the crucible with the igniter (carbon thread). After combustion and cooling down the system the solid raw product was collected. The product was later purified (leaching of Mg/MgO compounds using hot 3M HCl). The final sample contained mostly carbon (its content was analyzed using the elemental analysis). Both raw and purified products were examined using SEM (morphology) and XRD (phase composition) analyses.

## *3. Results and Discussion*

*3.1. System $Mg/C_6H_4(COOH)_2$*

The combustion of minerals was pre-tested (2 runs) with the magnesiothermic decomposition of the phthalic acid, a carbon-rich (58 wt% of C) commodity chemical produced on a large scale, following the reaction scheme

$$4\ Mg + C_6H_4(COOH)_2 = 8\ C + 4\ MgO + 3\ H_2$$

For a better conversion, 2-fold excess of a reducer (Mg powder, below 40 μm) was used. The operating parameters of combustions are shown in Table 1.

*Table 1. Combustion of $Mg/C_6H_4(COOH)_2$ mixture*

| Run # | 1 – 1 | 1 – 2 |
|---|---|---|
| Combustion atmosphere/ Starting pressure, MPa | Ar, 0.1 | Ar, 1.0 |
| Peak pressure, MPa | 1.1 | 3.2 |
| Starting mass of reactants, g | 6.55 | 7.21 |
| Mass of solid product, g | 6.08 | 6.57 |
| Mass decrease, % | 7.2 | 8.9 |
| Starting mass of raw product, g | 6.04 | 6.2 |
| Mass of purified product, g | 2.31 | 2.45 |
| Mass decrease, % | 61.8 | 60.5 |

The combustion was easily initiated and strongly exothermic reaction was accompanied by a distinct pressure increase. The mass decrease of reactants was relatively low (below 10%) thus confirming the desirable reaction scheme. Puffy, greyish/blackish product was collected and leached with HCl. Up to 40 wt% of the raw product was recovered as an insoluble blackish residue (carbon-containing phase). The change of the starting pressure does not seem to influence the process. Fig. 2 and 3 present the representative images (SEM observation) of the raw and purified products.

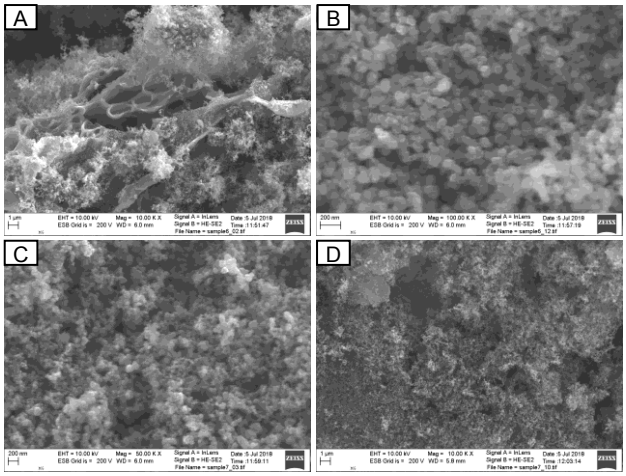


***Fig. 2**. Run # 1-1. SEM images of raw (A-B) and purified (C-D) product*

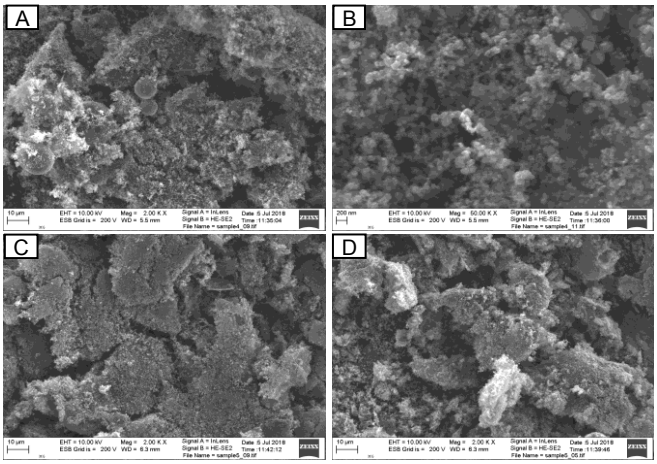


***Fig. 3**. Run # 1-2. SEM images of raw (A-B) and purified (C-D) product*

The raw product is dominated by nanometric crystallites of MgO, with some larger particles of un-reacted Mg. The leaching essentially does not change the product morphology thus confirming that the vast part of produced MgO is covered with a thin nanocarbon layer, insoluble in HCl. The EDX analyses of purified products fully confirmed that observation (Table 2).

*Table 2. The results of EDX analyses of purified products*

| Run # | 1 – 1 | 1 – 2 |
|---|---|---|
| C content, wt% | 61-63 | 72-75 |
| O content, wt% | 18-23 | 13-16 |
| Mg content, wt% | 15-19 | 10-11 |

The results of those reference combustions showed that magnesium effectively reduces oxygen-containing organic matter yielding the final nanopowder composed mostly of C (60-70 wt%). This nanocarbon material dominates the purified product which, however, still contains MgO nanocrystallites encapsulated in a carbon shell.

*3.2. System Mg/magnesite $MgCO_3$ (Szklary, Poland)*

The composition of magnesite (mostly nanometric powder, Fig. 4) was analyzed with EDX technique (the spectra not shown here). The results (C, Mg, O and Si content 7.7, 21.3, 49.8, and 20.3 wt %, respectively) confirmed that it is mostly composed of $MgCO_3$ with some silica/silicates admixtures, as expected for a mineral.

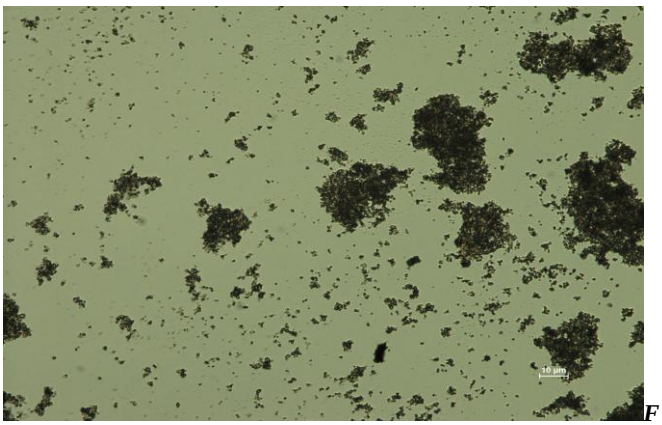

***Fig. 4**. Fine-grinded magnesite (Szklary, Poland)*

The mineral was reduced with magnesium (Mg powder, below 40 μm) following the reaction scheme

$$2\ Mg + MgCO_3 = C + 3\ MgO$$

This reaction can be, however, accompanied by the parallel thermal decomposition of magnesium carbonate with the evolution of carbon dioxide carrying away the carbon from the solid products

$$MgCO_3 \rightarrow MgO + CO_2$$

Thus, the final composition of the solid product is governed by the kinetics of both competing reactions. The operating parameters of all combustions (stoichiometric composition of reactants) are shown in Table 3. In runs 2-2 and 2-4 the starting mixture was additionally ball-milled (2 h) in hexane.

*Table 3. Combustion of Mg/magnesite mixture*

| Run # | 2 – 1 | 2 – 2 | 2 – 3 | 2 – 4 |
|---|---|---|---|---|
| Combustion atmosphere/ Starting pressure, MPa | Ar, 0.1 | Ar, 0.1 | Ar, 1.0 | Ar, 1.0 |
| Peak pressure, MPa | 0.4 | 0.3 | 1.9 | 1.9 |
| Starting mass of reactants, g | 5.47 | 3.46 | 6.91 | 3.38 |
| Mass of solid product, g | 5.24 | 3.16 | 6.07 | 3.16 |
| Mass decrease, % | 4.2 | 8.7 | 12.2 | 6.5 |
| Starting mass of raw product, g | 4.77 | 2.7 | 5.19 | 2.54 |
| Mass of purified product, g | 0.94 | 0.51 | 0.82 | 0.42 |
| Mass decrease, % | 80.3 | 81.1 | 84.2 | 83.5 |
| Combustion duration, sec | 2.52 | 3.34 | 1.3 | 2.27 |

The reaction mixture was easily and effectively combusted with a pressure jump caused by a heat-up of reactants and the evolution of hot gaseous by-products. The mass decrease of starting mixture was found to be within ca 10.0 wt%. Thus, one can conclude that the thermal pyrolysis of a carbonate (directly into MgO and $CO_2$) is responsible for the loss of only below 20 wt % of starting carbonate while its almost total conversion is dominated by a fast (well below 5 sec, Table 3) direct magnesiothermic reduction following the main reaction scheme. This conclusion was confirmed by the elemental analysis (C content) of reactants. Puffy, greyish/blackish product was collected and leached with HCl. The mass of purified product was monitored and compared to that of raw material. In agreement with the reduction stoichiometry up to 20 wt% of the raw product was insoluble (carbon phase). Neither the change of the starting pressure nor the prolonged milling in hexane influenced the process. Fig. 5 presents the representative images (SEM observation) of the reactants.

The starting reactants (A-B) are inhomogeneous mixture of micron-sized particles which, during the combustion, form mostly the conglomerates of nanosized MgO crystallites. Those are essentially removed during the acid leaching but the nanostructure of the solid residue (mostly carbon material) is still preserved. New structures are, however, also spotted in a purified product, i.e. nanowires (probably SiC[8]) and layered graphene-related nanomaterial. XRD spectra of selected samples are shown in Fig. 6.

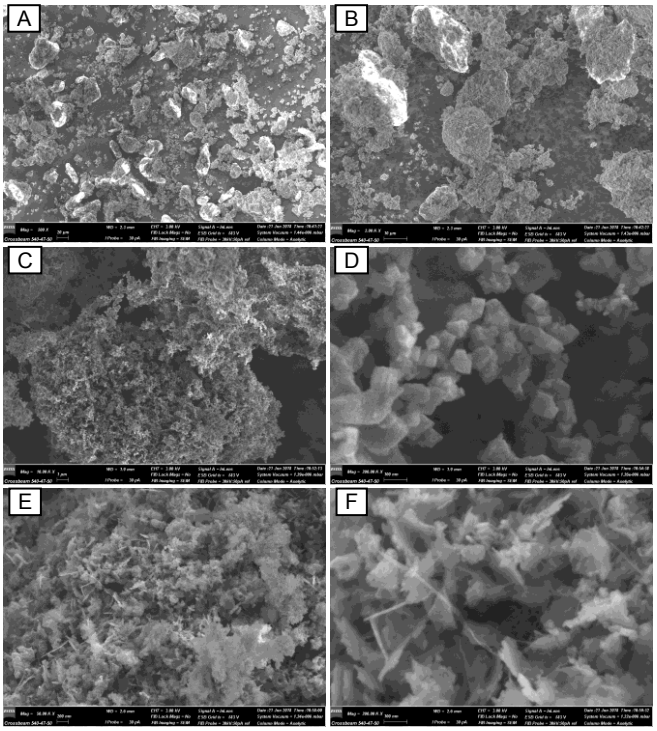


**Fig. 5**. *Run # 2-4. SEM images of starting mixture (A-B), raw (C-D) and purified (E-F) product*

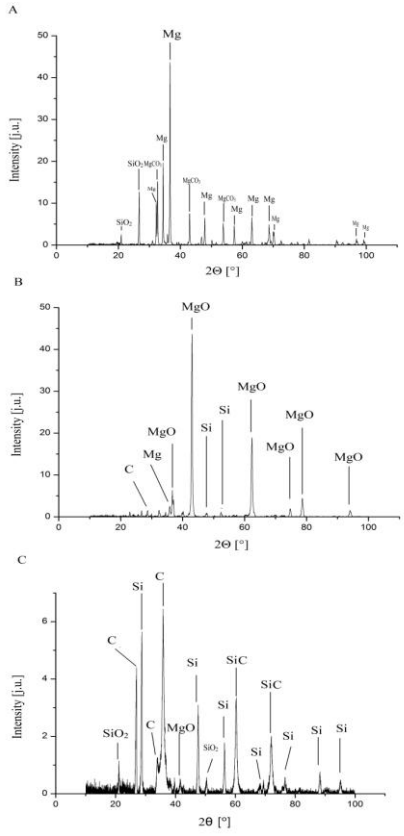


***Fig. 6***. *XRD spectra (run # 2-2) of selected samples: A – starting mixture; B – raw product; C – purified product*

Mg and $MgCO_3$ are the main components of starting mixture (A) with some silica/silicates as the minor impurity of a magnesite. The XRD spectrum of the raw product (B) is completely different thus confirming the deep transformation of the magnesite during the reduction. MgO dominates the product with some traces of un-reacted Mg. Carbon phase is also present while silicon elemental phase presence is the result of either silica/silicates or crucible material magnesiothermic reduction. Carbon phase dominates the purified product (C) while $SiO_2$, Si, MgO, and SiC are the side admixtures still present in the sample. The composition of the purified product confirms that alkaline components have not been removed during the acid leaching while SiC was formed from elemental silicon and carbon which dominates the reactants.

The EDX analyses of a purified product fully confirmed that finding with the following content of the main elements: C – 51.7, Mg – 0.9, O – 16.5, and Si – 30.9 wt %.

*3.3. System Mg/dolomite (Kavre,Nepal)*

Powdered dolomite (calcium magnesium carbonate) was also reduced with Mg metal via combustion synthesis following the reaction scheme

$$4\ Mg + CaMg(CO_3)_2 = 2\ C + CaO + 5\ MgO$$

Again, the parallel high-temperature thermal decomposition of this complex carbonate is also possible. All combustions were easily initiated and greyish/blackish fine powder was collected for the purification and the following analyses. The operational parameters of those combustions are shown in Table 4.

***Table 4.*** *Combustion of Mg/dolomite mixture*

| Run # | 3 – 1 | 3 – 2 |
|---|---|---|
| Combustion atmosphere/ Starting pressure, MPa | Ar, 0.1 | Ar, 1.0 |
| Peak pressure, MPa | 1.0 | 2.0 |
| Starting mass of reactants, g | 7.11 | 10.05 |
| Mass of solid product, g | 7.04 | 9.96 |
| Mass decrease, % | 1.0 | 0.9 |
| Starting mass of raw product, g | 6.78 | 9.61 |
| Mass of purified product, g | 0.71 | 1.3 |
| Mass decrease, % | 89.5 | 86.5 |

The very law mass decrease (ca 1 wt%) of solid reactants during combustion confirms practically the only reaction channel as shown in the desired scheme above. Above 10 % of the solid product (nanocarbon phase) was recovered after the purification stage. The change of the starting combustion pressure thus not seem to influence the process confirming its course entirely in solid-liquid phase. The representative SEM images of the selected products are shown in Fig. 7.

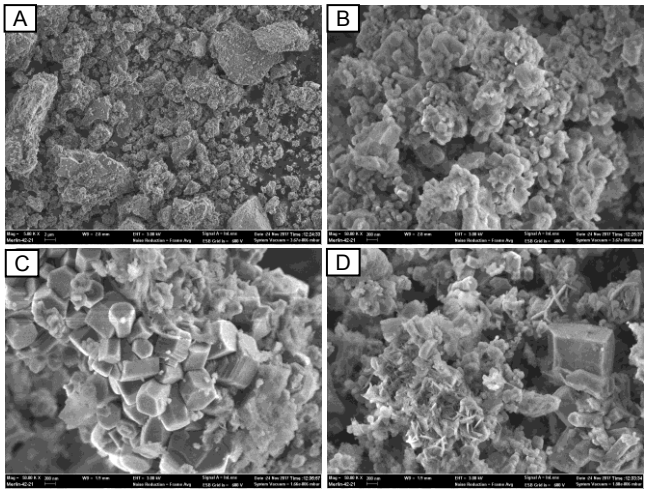


***Fig. 7****. Run # 3-2. SEM images of raw (A-B) and purified (C-D) product*

The raw product (A-B) is an inhomogeneous mixture of un-reacted micron-sized Mg particles and agglomerates of nanostructured matter (mostly MgO). The purified blackish product (C-D) contains mostly MgO nanocrystallites covered with a thin carbon layer. Some intriguing one-dimensional and layered structures (nanocarbons?) can also be spotted in the product.

The non-linear course of combustion synthesis allows to obtain a nanomaterial, which may be impossible to obtain by conventional methods. The SHS processes, however, are susceptible to changing initial conditions and phase transformations of reactants disturbing heat and mass transport in the system. The consequence of such phenomena causes a difficulty in process modeling, which makes it impossible to predict the final synthesis product. The attempt to optimize the process involves time-consuming parametric studies, which makes the calculations of equilibrium thermodynamics often too much simplified. Lack of sufficient information on transient compounds prevents the modeling of process kinetics for higher orders of reaction. In the answers to these limitations the methods arose that investigate processes based on propagation combustion wave, using fractal analysis or identification of compounds at their stage follow-up reactions using time-variable analysis of the light signal on based on registered images.

In the combustion synthesis process, the heated reactants emit the radiation that is responsible for variable light signal. Optical and /or spectral registration of such a signal can be used in the process diagnostics to measure the duration of the flash or other parameters accompanying combustion.

The flash sequences for the synthesis # 2-1 and # 2-3 were photographically recorded by means of a Pentax digital camera with HD resolution of 1920x1800 and speed of 30 frames per second (duration of one frame is about 0.03s). Based on divided and selected frames, combustion maps have been made for each test from photos arranged in the progress sequence (from left to right). On the basis of these data it was possible to determine the flash time, maxima, qualitative mileage and occurrence of follow-up reactions. Fig. 8 and Fig. 9 present representative combustion maps for those synthesis with an initial pressure of 0.1 MPa and 1.0 MPa.

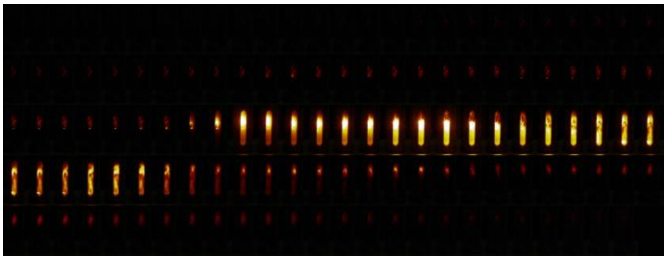

***Fig.*** *8. Combustion map for run # 2 –*

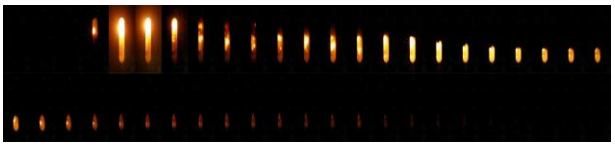

***Fig.*** *9. Combustion map for run # 2-3*

For the run # 2-1 the flash lasted about 3.34s and the maximum reached after 0.81s. The observed extended flash-out times were slower and the passage of the combustion wave was smoother than in run # 2-3. For the run # 2-3 the flash lasted about 1.30s and the maximum reached after 0.07s. A rapid flash was observed and a greater scattering of the solid product was found within the reactor.

## *4. Conclusions*

Carbon-bearing synthetic (phthalic acid) compound and natural minerals (magnesite of Polish and dolomite of Nepal origin) were processed via fast magesiothermic and autothermic reduction. The resulting solid product was chemically (wet chemistry) purified to yield mostly carbon-containing nanomaterial. The presence of silica/silicates in a purified product calls for the improvement of the purification protocol. Thus, the raw product should be leached not

only with HCl but also with NaOH. The produced nanosized carbon material should present the prospective applications, i.e. as an adsorbent, substrate for catalyst, and a component of electrodes in electrochemistry (lithium ion batteries and fuel cells).

## *5. References*

1. Tiwari S.K., V. Kumar, A. Huczko, R. Oraon, A. De Adhikari, G.C. Nayak (2016) Magical Allotropes of Carbon: Prospects and Applications. Critical Reviews in Solid State Materials Science 41: 257–317

2. Kroro H.W., J. R. Heath, S. C. O'Brien, R. F. Curl & R. E. Smalley (1985) $C_{60}$: Buckminsterfullerene. Nature 318: 162–163

3. Iijima, S. (1991) Synthesis of Carbon Nanotubes. Nature 354: 56-58

4. Novoselov K.S., A. K. Geim, S. V. Morozov, D. Jiang, Y. Zhang, S. V. Dubonos, I. V. Grigorieva, A. A. Firsov (2004) Electric Field Effect in Atomically Thin Carbon Films. Science 306: 666-669

5. Zhao Y., X.G. Li , X. Zhou, Y.N. Zhang (2016) Review on the Graphene Based Optical Fiber Chemical and Biological Sensors. Sensors and Actuators B: Chemical 231: 324-340

6. Dyjak S., W. Kiciński, A. Huczko (2015) Thermite-driven Melamine Condensation to CxNyHz Graphite Ternary Polymers: Towards an Instant, Large-scale Synthesis of g-$C_3N_4$. J. Mater. Chem. A 3: 9621-9631

7. Manning T.J., M. Mitchell, J. Stach, T. Vickers (1999) Synthesis of Exfoliated Graphite from Fluorinated Graphite using an Atmospheric-pressure Argon Plasma. Carbon 37: 1159-1164

8. Morsi K. (2012) The Diversity of Combustion Synthesis Processing: a Review. J. Mater. Sci. 47: 68-92

9. Huczko, A., H. Lange, G. Chojecki, S. Cudziło, Y.Q. Zhu, H.W. Kroto, D.R.M. Walton (2003) Synthesis of Novel Nanostructures by Metal-Polytetrafluoroethene Thermolysis. J. Phys. Chem. B 107: 2519-2524

10. Dąbrowska A., A. Huczko, M. Soszyński, B. Bendjemil, F. Micciulla, I. Sacco, L. Coderoni, S. Bellucci (2011) Ultra-fast Efficient Synthesis of One-dimensional Nanostructures. Phys. Status Solidi B 248: 2704-2707

11. Dąbrowska A., A. Huczko, S. Dyjak (2012) Fast and Efficient Combustion Synthesis Route to Produce Novel Nanocarbons.Phys. Status Solidi B 249: 2373-2377

12. Huczko, A., A. Dąbrowska, O. Łabędź, M. Soszyński, M. Bystrzejewski, P. Baranowski, R. Bhatta, B. Pokhrel, B.P. Kafle, S. Stelmakh, S. Gierlotka, S. Dyjak (2014) Facile and Fast Combustion Synthesis and Characterization of Novel Carbon Nanostructures. Physica Status Solidi B 251: 2563-2568

13. Huczko A., O. Łabędź, A. Dąbrowska, M. Kurcz, M. Bystrzejewski, H. Lange, P. Baranowski, L. Stobiński, A. Małolepszy, A. Okotrub, M. Soszyński (2015) Efficient One-pot Combustion Synthesis of Few-layered Graphene. Physica Status Solidi B 252: 2412-2417

14. Dyjak S., W. Kiciński, M. Norek, A. Huczko, O. Łabędź, B. Budner, M. Polański (2016) Hierarchical, Nanoporous Graphenic Carbon Materials Through an Instant, Self-sustaining Magnesiothermic Reduction. Carbon 96: 937-946